

CHAPTER 69

A FIELD EXPERIMENT ON THE INTERACTIONS WAVES-REFLECTING WALL

Paolo Boccotti

Department of Fluid Mechanics and Offshore Engineering
University of Reggio Calabria
Via E. Cuzzocrea, 48 - 89100 Reggio Calabria - Italy
Fax. +39 965 875220

Abstract

A special reflecting wall 12 m long and 2.1 m high was built off the beach at Reggio Calabria, and 30 wave gauges were assembled before the wall and were connected to an electronic station on land. It was possible to observe the reflection of wind waves generated by a very stable wind over a fetch of 10 Km. The experiment aimed to verify the general closed solution for the wave group mechanics (Boccotti, 1988, 1989), for the special case of the wave reflection.

1 Introduction

Starting on 1990, a few small scale field experiments were executed off the beach at Reggio Calabria on the eastern coast of the Straits of Messina. The original aim was to verify the closed solution for the mechanics of the highest 3-D wave groups in the wind generated sea states (Boccotti, 1988, 1989).

The tide excursion in the area is very small and a local wind often remains constant from the North West for several consecutive days. After two days of NW wind, the Southerly swells vanish and the sea states in front of Reggio Calabria consist of pure wind waves with significant height typically within 0.2 and 0.4 m and dominant period within 1.8 and 2.5 s.

Because of the small wave size and of the very small tide excursion, it is possible to operate like in a big wave tank. Moreover, the water is exceptionally clear because of the Strait current which flows for about one half an hour in 12 hours. The clearness of the water enables

underwater works of high precision.

The first experiment (May, 1990) was concerned with the progressive waves on deep water. An array of nine wave gauges and nine pressure transducers supported by vertical iron piles provided space-time information on waves generated over a fetch of approximately 10 Km. It was confirmed that the general 3-D configuration of the extreme wave groups was consistent with the theoretical predictions (Boccotti et al., 1993-a).

Given that the closed solution for the mechanics of the highest wave groups holds (to the Stokes first order) for an arbitrary shape of the solid boundary, it particularly predicts the reflection of a 3-D wave group by a wall. Thus, a second experiment was executed on May, 1991 with the main purpose to verify whether the reflection of the 3-D wave groups was consistent with the theoretical prediction. Here a few results of this verification are shown. Previously, the experiment's data were used by Boccotti et al. (1993.b) to test a few predictions on the variations of wave energy and band-width with distance from the wall.

2 The closed solution for the mechanics of the wave groups on the sea surface (Boccotti, 1988, 1989)

Let us consider a random wind-generated sea state assumed Gaussian (Longuet-Higgins, 1963 and Phillips, 1966). The extreme wave events have been shown by the writer to occur in a well defined way that can be specified in terms of the autocovariance function. The theory admits that the random wave field is generally non-homogeneous: it can be homogeneous like in an open sea or non-homogeneous like before a reflecting wall.

Specifically, if the extreme wave crest occurs at $\underline{x}_0 = (x_0, y_0)$ at time t_0 , with a crest-to-trough height of H , the mean surface configuration in space and time is given by

$$\eta_c(\underline{x}_0 + \underline{X}, t_0 + T) = \frac{H}{2} \left\{ \frac{\Psi(\underline{X}, T) - \Psi(\underline{X}, T - T^*)}{\Psi(\underline{0}, 0) - \Psi(\underline{0}, T^*)} \right\} \quad (2.1)$$

where Ψ is the autocovariance function of the surface displacement of the random wave field

$$\Psi(\underline{X}, T) = \langle \eta(\underline{x}_0, t) \eta(\underline{x}_0 + \underline{X}, t + T) \rangle \quad (2.2)$$

and T^* is the abscissa of the absolute minimum of the autocovariance function $\Psi(\underline{0}, T)$, which is assumed to exist and to be the first minimum after $T=0$. Superimposed on the deterministic form (2.1) is of course the random noise of the residual wave field, but when $H/\sigma(\underline{x}_0)$ is large ($\sigma(\underline{x}_0)$ being the r.m.s. wave elevation at location \underline{x}_0), the variations in the actual sea surface configuration surrounding \underline{x}_0, t_0 are small compared with η_c itself.

Associated with the configuration (2.1) is a distribution of velocity

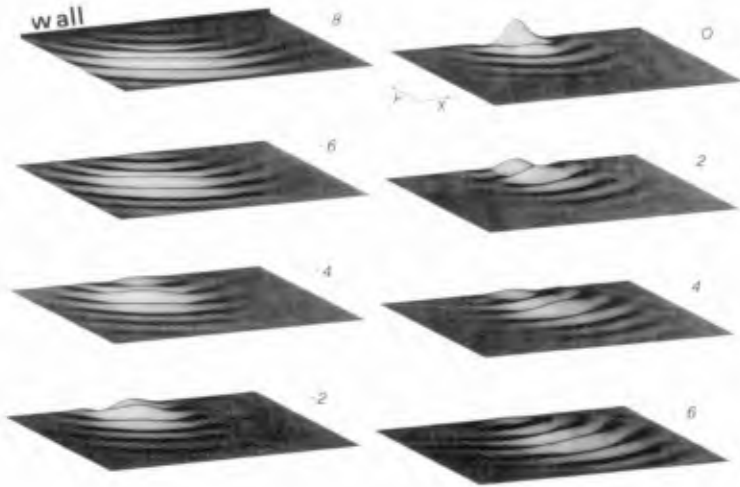


Fig.1 Occurrence of a wave of given very large height at a reflecting wall. The wall is along the upper x-parallel side of the framed rectangle, and the interval between two consecutive configurations is of 2 Td (Td being the dominant period of the random sea state). The wave group impacts the wall, at the apex of the development stage (minimum width of the wave front and maximum height of the central wave), it is reflected mirrorwise and goes back seaward.

potential in the water, which to the lowest order in a Stokes expansion is given by

$$\phi_c(\underline{x}_o + \underline{X}, z, t_o + T) = \frac{H}{2} \left\{ \frac{\Phi(\underline{X}, z, T) - \Phi(\underline{X}, z, T - T')}{\Psi(\underline{0}, 0) - \Psi(\underline{0}, T')} \right\} \quad (2.3)$$

where

$$\Phi(\underline{X}, z, T) = \langle \eta(\underline{x}_o, t) \phi(\underline{x}_o + \underline{X}, z, t + T) \rangle. \quad (2.4)$$

The theory holds for arbitrary solid boundary conditions, and it can be formally proved that deterministic functions η_c and ϕ_c satisfy the Stokes equations to the first order as well as an arbitrary set of solid boundary conditions, if random functions η and ϕ satisfy those equations and boundary conditions. Note that the hypothesis that $H/\sigma(\underline{x}_o)$ is large is not necessarily inconsistent with the use of the lowest order (linear) terms in a Stokes expansion, provided H remains small with respect to the wave length and the water depth.

The covariances (2.2) and (2.4) can be readily obtained from the directional frequency spectrum of the random sea state. In the case that the random sea state interacts with some obstacle, e.g. with a

reflecting wall, the covariances can be obtained from the directional frequency spectrum of the wave field that there would be if the obstacle was not there (see Appendices A and B).

From equation (2.1) we find that a wave of given very large height H at a location x_0 in an open sea occurs because a well defined wave group transits that location, when it is at the apex of its development stage. A few 3-D pictures of the wave group can be seen in the papers of Boccotti (1988) and (1989) and of Boccotti et al. (1993-a). The basic phenomena that occur during the course of evolution of the group are not dependent on the detailed shape of the wave spectra, though the shape of the group does vary somewhat. Specifically, the wave group has always a development stage in which the height of its central wave grows to a maximum and the width of the wave front reduces to a minimum. Then a decay stage follows with the opposite features. The individual waves have a propagation speed greater than the envelope so that each wave crest is born at the tail of the group, grows to a maximum when it reaches the central position, and then dies at the head of the group.

From equation (2.1) we find also that a wave of given very large height at a location x_0 of a reflecting wall, occurs because a wave group impacts the wall, when it is at the apex of the development stage -see Figure 1-. Then we find that a very high wave at a location x_0 far from the wall occurs because of the collision of two wave groups -the first one approaching the wall, and the second one going back seaward after having been reflected.

Finally, equation (2.1) shows that a very high wave at a location x_0 behind a wall (we mean "very high with respect to the mean wave height at this location") occurs because a wave group targets on the wall-end, and, after the impact with the wall, one half of the wave front goes on and penetrates into the shadow cone. The relevant 3-D pictures can be seen in the papers of Boccotti (1988).

3 The experiment of May 1991 off the beach at Reggio-Calabria

Eq.(2.1) holds not only for the surface waves but also for the pressure head waves at some fixed depth. In this case, η is to be intended as the fluctuating pressure head at the fixed depth. This property is a consequence of the fact that, to the Stokes first order, the fluctuating pressure head at some fixed depth represents a stationary Gaussian process of time like the surface displacement. Therefore, aiming to test eq.(2.1), the decision was taken to deal with the pressure head waves at a fixed depth, given that the fluctuating pressure head can be measured by transducers of high precision and low cost.

A set of pressure transducers was assembled before (seaward) a special upright reflecting wall 12 m long and 2.1 m high with a rubble mound .2 m high. The structure consisted of a steel truss whose stability was ensured by a dead weight of pig iron discs, and the reflecting plane was formed by aluminium panels with a thickness of .05 m.

The transducers were supported by three horizontal beams .6 m below

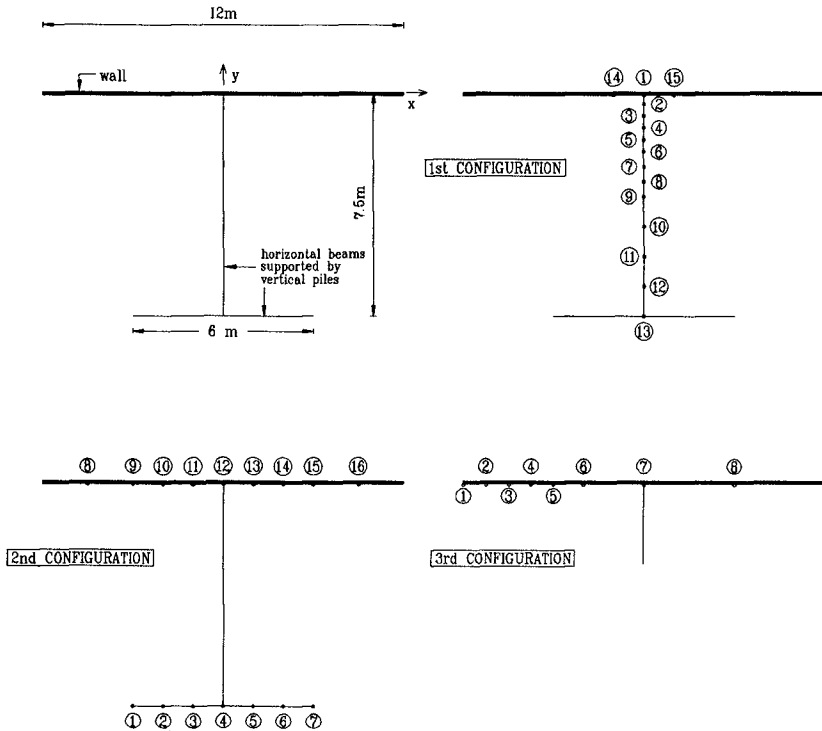


Fig.2 Plan view of the pressure transducers before the wall.

the mean water level -see Figure 2-. The average bottom depth in the area covered by the gauges was of 2.0 m. Both the horizontal beams and the supporting piles were designed to get an high degree of stiffness as well as a small section, and in particular each upright pile of the diameter of .05 m was stiffened by four small steel cables. The pressure transducers were connected by submarine cables to an A/D converter unit in an onshore building and the sampling rate was 10 hz. Besides the pressure transducers, an ultrasonic wave probe far from the wall provided information on the undisturbed waves.

Three different configurations of the gauges were assembled during the experiment -see Figure 2-. A set of 9 records was obtained with the first configuration, and sets of 27 and of 16 records were obtained respectively with the second and with the third configuration. The total number of the records was then of 52, each of 9 minutes and containing 250 to 300 dominant waves. The significant height H_s ranged within .17 and .42m and the dominant period T_d within 1.9 and 2.6s.

4 A few results of the experiment

The covariances can be found directly from the measurements by cross-correlation of the time series obtained at the discrete measurement locations and if an extreme wave of the pressure head, with a crest-to-trough height of H , is encountered at one such location, the time history of the expected pressure head configuration at this and the other locations can be obtained from (2.1).

With x_0 taken as location 1 at the wall-center (first configuration of the gauges), the vectors X were specified by the relative locations of the other gauges. The time series data of record 17 provided measured auto-covariances as a function of T for the various gauge locations and these were used *without smoothing* on the right hand side of equation (2.1) to estimate $\eta_c(t_0+T)$ at these locations in an extreme wave. The results are shown in Figure 3.

The covariances were found also from a theoretical spectrum. The classic JONSWAP frequency spectrum (Hasselmann et al., 1973) and the spreading direction function of Mitsuyasu et al. (1975) were assumed for the two dimensional spectrum of the wave field that there would be if the wall was not there. The spreading direction parameter n_0 of Mitsuyasu et al. was taken equal to 20, that is the suggested value for the conditions of our experiment: fetch 10000 m, wind velocity 7-8 m/s. The dominant wave period and the dominant direction were given the values of record 17. The dominant period was of 1.9 s. The direction was estimated accurately since the front of wave A at the traverse of locations 14-1-15 (at the wall) proves to be nearly straight. The relative phases indicated an angle of incidence of 13°.

The substitution of the theoretical covariances in equation (2.1) leads to Figure 4. Like Figure 3, this shows the expected waves in the time domain, at the various gauge locations, if a wave of given very large height H occurs at location 1 at the wall-center, with the first configuration of the gauges. The likeness of the two figures is amazing - figure 3 was obtained from the time series data, while figure 4 was obtained from a theoretical spectrum!

In the figures, A represents the wave of given very large height H at location 1, B, C and D are the waves immediately before this one, and B', C', D' are the waves immediately after A. At the wall, A occupies the envelope center.

The wave height exhibits a local minimum (node) at location 5, because the waves approaching the wall overlap the reflected waves in phase opposition. Then, a local maximum of the wave height (antinode) takes place at location 8, where the waves overlap themselves in phase coherence. The dominant wave length L_d was of nearly 6 m, so that the node was at $\frac{1}{4}L_d$ from the wall, and the antinode was at $\frac{1}{2}L_d$ from the wall. At the antinode, two waves of the same height occupy the envelope center, the first one is the overlap of wave A approaching the wall and of preceding wave B going back after having been reflected; the second one is the overlap of wave A going back seaward and of succeeding wave B' approaching the wall. At greater distances from the wall, nodes and antinodes tend to disappear because the central waves of the group

FROM CROSS-CORRELATION OF THE TIME SERIES DATA

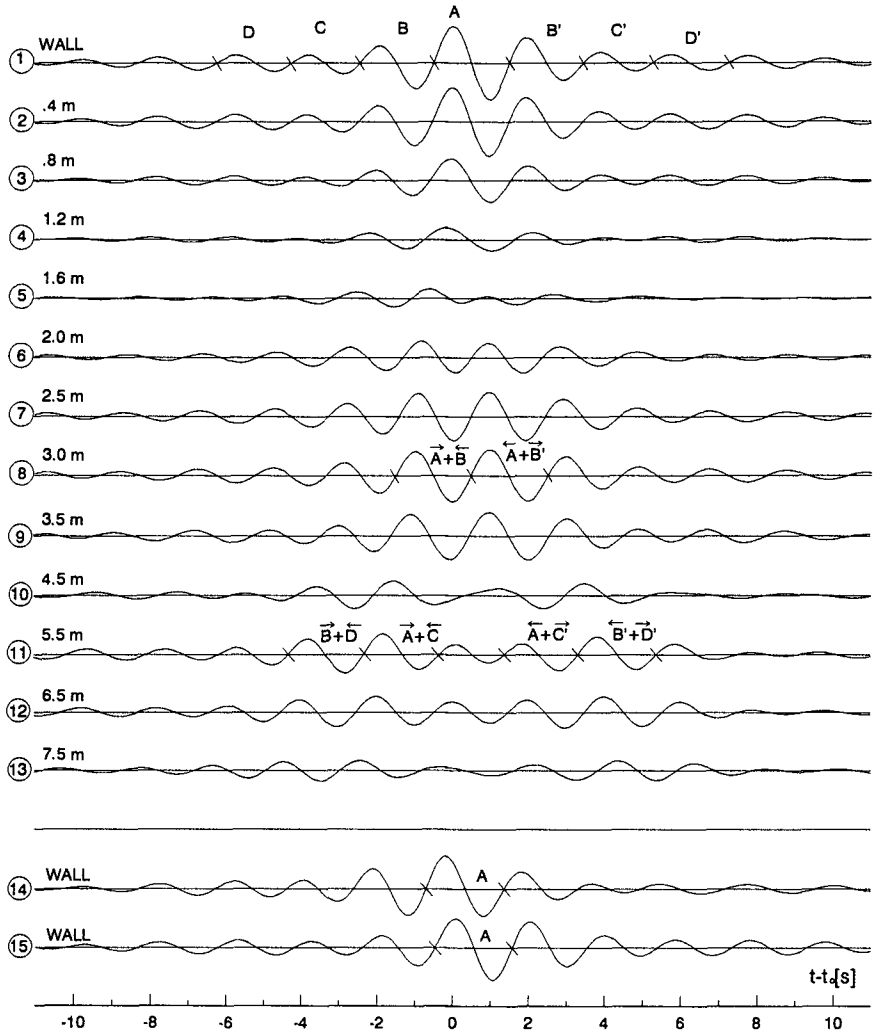


Fig.3 Expected waves at the various gauge locations if a wave of given very large height H occurs at location 1 (wall-center) with the first configuration of the gauges. Calculation from equation (2.1), directly with the time series data of record 17, without smoothing.

FROM THE JONSWAP SPECTRUM

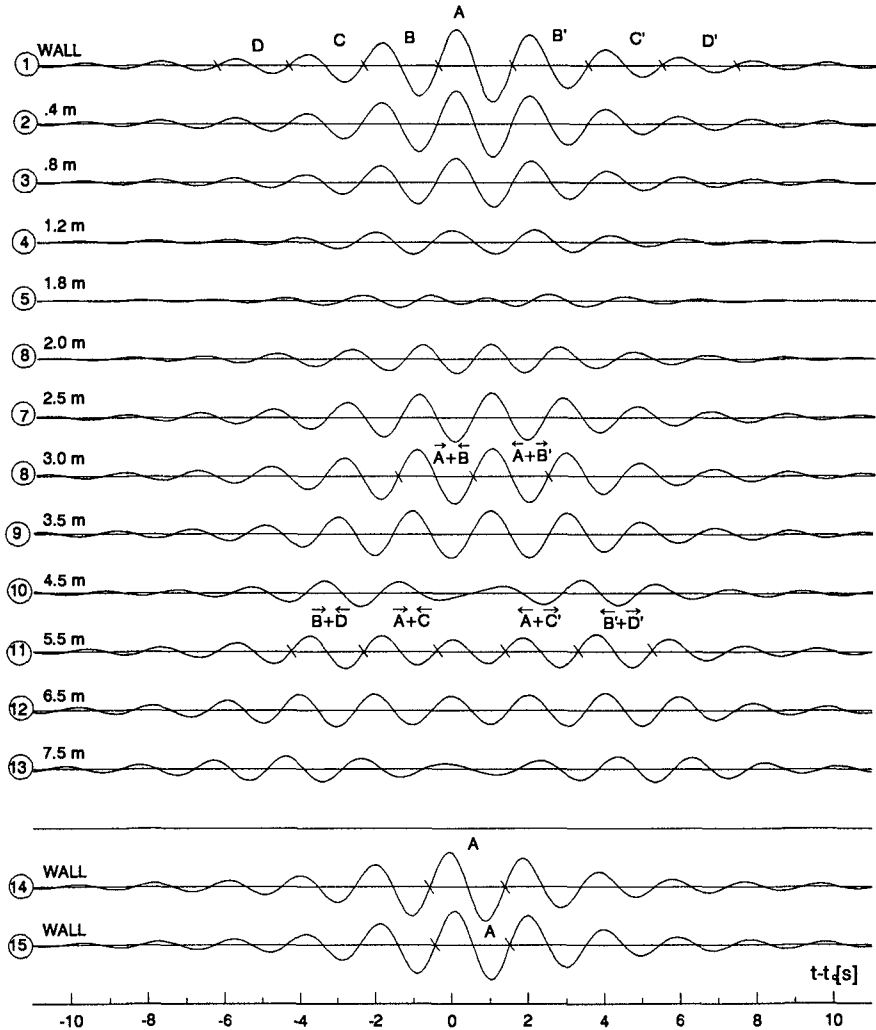
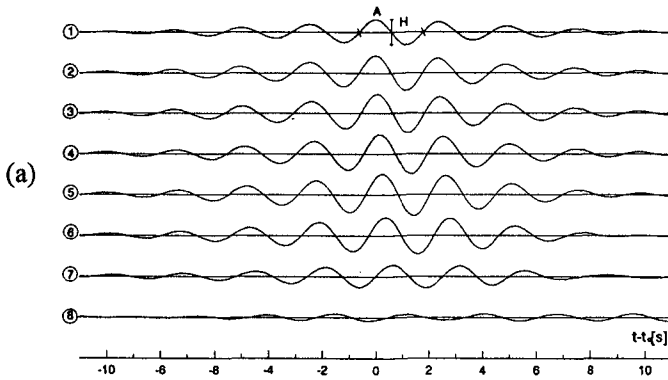


Fig.4 Expected waves at the various gauge locations if a wave of given very large height H occurs at location 1 (wall-center) with the first configuration of the gauges. Calculation from equation (2.1), with the JONSWAP spectrum and the spreading direction function of Mitsuyasu et al.(1975).

FROM CROSS-CORRELATION OF THE TIME SERIES DATA



FROM THE JONSWAP SPECTRUM

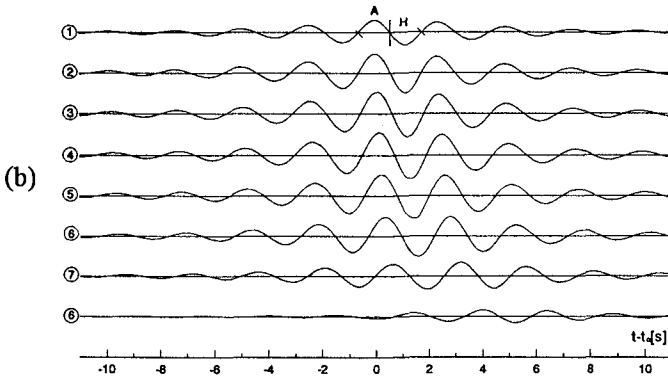


Fig.5 Expected waves at the various gauge locations if a wave of given very large height H occurs at location 1 (wall-end) with the third configuration of the gauges. Calculation from eq.(2.1). Panel (a): covariances obtained by cross-correlation of the time series data of record 30. Panel (b): covariances obtained with the JONSWAP spectrum and the spreading direction function of Mitsuyasu et al.(1975).

do not overlap themselves, and it is possible to distinguish the wave group approaching the wall from the wave group going back seaward. In particular, at location 13, which is the most remote from the wall, we see the wave group approaching the wall, then a short calm, then the wave group going back.

Fig.5 shows the expected time histories at the locations of the third gauge configuration if a wave of fixed very large height H occurs at the wall-end (H is intended to be very large with respect to the

mean wave height at the wall-end). The calculation was made by means of eq.(2.1). The covariances used for Fig.5.a were obtained by cross-correlation of the time series of record 30, while the covariances used for Fig.5.b were obtained from a theoretical spectrum (see Appendix B). The general form of the theoretical spectrum was that used for Fig.4, and the dominant wave period and wave direction were given the values of record 30. The dominant period was 2.5 s and the angle of the dominant wave direction with the wall-orthogonal was 22°.

A very high wave at the wall-end, with a very high probability, occurs because the front center of a wave group targets on the wall-end. For this reason, the wave height along the wall, on the one hand has to decrease starting on the wall-end because of the increasing distance from the front center, and on the other hand it has to increase because of the raising produced by the wall. The result is that a local maximum of the wave height takes place at some distance from the wall-end. This observation should permit to understand the overall configurations of figures 5.a and 5.b. These configurations are strongly similar to each other, and particularly we can see, in both two the figures, that the local maximum of the wave height falls within locations 4 and 5, at nearly $\frac{1}{3}$ wave length from the wall-end.

Figs.3 and 5.a prove that the wind wave field has something like a "genetic code" showing what essentially happens if a very high wave occurs at any fixed location. Given that x_0 can be anyone of the gauge locations, we drew a number of pictures like Figs.3 and 5.a from each record, and the expected time histories were always smooth and consistent with one another as in the figures shown in this paper. Although the records from single realizations of very high waves were more irregular than the expected profiles, the essential features of these profiles were still evident and provided good support for the theoretical connection. This topic is dealt with in a forthcoming paper giving also a more simple formal proof of the theory.

Appendix A. Autocovariance of the wind waves being subject to reflection A.a Surface waves

According to the theory of the sea waves to the Stokes first order (Longuet-Higgins, 1963), the surface displacement of a progressive wave field is

$$\eta(x, y, t) = \sum_{i=1}^N \alpha_i \cos(k_i x \sin \theta_i + k_i y \cos \theta_i - \omega_i t + \epsilon_i), \quad k_i \tanh(k_i d) = \omega_i^2 / g. \quad (A.1)$$

where it is assumed that number N is very large, phases ϵ_i are distributed purely at random in $(0, 2\pi)$, frequencies ω_i are different from one another. Then it is assumed that α_i , ω_i and θ_i (this being the angle of wave direction and y-axis) are such as to form a directional frequency spectrum

$$S(\omega, \theta) \delta\omega \delta\theta = \sum_i \frac{1}{2} \alpha_i^2 \quad \text{for } i \text{ such that } \omega < \omega_i < \omega + \delta\omega \text{ and } \theta < \theta_i < \theta + \delta\theta. \quad (A.2)$$

If a vertical reflecting wall is put along the x-axis (line y=0), random wave field (A.1) takes on the form (Boccotti, 1988)

$$\eta(x, y, t) = 2 \sum_{i=1}^N \alpha_i \cos(k_i x \sin \theta_i - \omega_i t + \epsilon_i) \cos(k_i y \cos \theta_i). \quad (A.3)$$

From this equation of the surface displacement, and definition (2.2) of the autocovariance, we have

$$\Psi(\underline{X}, T) = 4 \sum_{i=1}^N \sum_{j=1}^N \alpha_i \alpha_j \cos(k_i y_o \cos \theta_i) \cos[k_j (y_o + Y) \cos \theta_j] \cdot \langle \cos(k_i x_o \sin \theta_i - \omega_i t + \epsilon_i) \cos(k_j x_o \sin \theta_j - \omega_j t + \epsilon_j + k_j X \sin \theta_j - \omega_j T) \rangle, \quad (A.4)$$

where

$$\underline{x}_o = (x_o, y_o), \quad \underline{X} = (X, Y), \quad (A.5)$$

and the angle brackets denote an average with respect to time t. Eq.(A.4) is reduced to

$$\Psi(\underline{X}, T) = 4 \sum_{i=1}^N \frac{1}{2} \alpha_i^2 \cos(k_i X \sin \theta_i - \omega_i T) \cos(k_i y_o \cos \theta_i) \cos[k_i (y_o + Y) \cos \theta_i], \quad (A.6)$$

and with the definition (A.2) of $S(\omega, \theta)$

$$\Psi(\underline{X}, T) = 4 \int_0^\infty \int_0^{2\pi} S(\omega, \theta) \cos(k X \sin \theta - \omega T) \cos(k y_o \cos \theta) \cdot \cos[k (y_o + Y) \cos \theta] d\theta d\omega. \quad (A.7)$$

Thus, if we specify function $S(\omega, \theta)$ and location \underline{x}_o we can evaluate the autocovariance. Note that eq. (A.7) depends on y_o but does not depend on x_o . This is a consequence of the fact that the wall is assumed to be very long, so that the autocovariance generally changes with distance $|y_o|$ from the wall, but does not change with position x_o along the wall.

A.b Pressure head waves

In this section $\eta(x, y, t)$ is intended to be the fluctuating pressure head at some fixed depth z_o . Before a long reflecting wall, this is given by

$$\eta(x, y, t) = 2 \sum_{i=1}^N \alpha_i \frac{\cosh k_i (d + z_o)}{\cosh k_i d} \cos(k_i x \sin \theta_i - \omega_i t + \epsilon_i) \cos(k_i y \cos \theta_i), \quad (A.8)$$

so that the autocovariance (2.2) turns out to be

$$\Psi(\underline{X}, T) = 4 \int_0^\infty \int_0^{2\pi} S(\omega, \theta) \frac{\cosh^2 k (d + z_o)}{\cosh^2 k d} \cos(k X \sin \theta - \omega T) \cos(k y_o \cos \theta) \cdot \cos[k (y_o + Y) \cos \theta] d\theta d\omega. \quad (A.9)$$

This equation was used to obtain Fig.4.

Appendix B. Autocovariance of the wind waves being subject to diffraction

Near the wall-end, a more appropriate theory is that of the semi-infinite breakwater. If a semi-infinite breakwater is put along the x-axis, random wave field (A.1) takes on the form

$$\eta(r, \alpha, t) = \sum_{i=1}^N \alpha_i [F(r, \alpha; \omega_i, \theta_i) \cos(\omega_i t + \epsilon_i) + G(r, \alpha; \omega_i, \theta_i) \sin(\omega_i t + \epsilon_i)], \quad (B.1)$$

where r, α are polar coordinates with origin at the breakwater-end ($\alpha = 0$ at the protected wall, $\alpha = 2\pi$ at the wave beaten wall) and $F(r, \alpha; \omega, \theta)$ and $G(r, \alpha; \omega, \theta)$ are the functions of Penny and Price (1952) for a wave whose angular frequency is ω and whose direction makes an angle θ with the wall-orthogonal. If we define

$$\underline{x}_o = (r_o, \alpha_o) \quad , \quad \underline{x}_o + \underline{X} = (r, \alpha), \quad (B.2)$$

from general eq. (2.2) of the autocovariance we have

$$\Psi(\underline{X}, T) = \sum_{i=1}^N \sum_{j=1}^N a_i a_j \langle [F_i(r_o, \alpha_o) \cos(\omega_i t + \epsilon_i) + G_i(r_o, \alpha_o) \sin(\omega_i t + \epsilon_i)] \cdot [F_j(r, \alpha) \cos(\omega_j t + \epsilon_j + \omega_j T) + G_j(r, \alpha) \sin(\omega_j t + \epsilon_j + \omega_j T)] \rangle, \quad (B.3)$$

where, for simplicity, we have used the compact notation

$$F_i(r, \alpha) = F(r, \alpha; \omega_i, \theta_i). \quad (B.4)$$

Eq. (B.3) is reduced to

$$\Psi(\underline{X}, T) = \sum_{i=1}^N \frac{1}{2} a_i^2 \{ [F_i(r_o, \alpha_o) F_i(r, \alpha) + G_i(r_o, \alpha_o) G_i(r, \alpha)] \cos \omega_i T + [F_i(r_o, \alpha_o) G_i(r, \alpha) - G_i(r_o, \alpha_o) F_i(r, \alpha)] \sin \omega_i T \}, \quad (B.5)$$

and from the definition (A.2) of $S(\omega, \theta)$

$$\Psi(\underline{X}, T) = \int_0^{\infty} \int_0^{2\pi} S(\omega, \theta) \{ [F(r_o, \alpha_o; \omega, \theta) F(r, \alpha; \omega, \theta) + G(r_o, \alpha_o; \omega, \theta) G(r, \alpha; \omega, \theta)] \cos \omega T + [F(r_o, \alpha_o; \omega, \theta) G(r, \alpha; \omega, \theta) - G(r_o, \alpha_o; \omega, \theta) F(r, \alpha; \omega, \theta)] \sin \omega T \} d\theta d\omega. \quad (B.6)$$

This is the autocovariance of the surface waves. Then, autocovariance of the pressure head waves at some fixed depth z_o has one more factor in the integral. This is

$$\cosh^2 k(d + z_o) / \cosh^2 kd.$$

Eq. (B.6) with this additional factor was used to obtain Fig.5.b.

References

- Boccotti P., 1988, Refraction, reflection and diffraction of irregular gravity waves, Excerpta of the Italian Contribution to the Field of Hydraulic Engng., vol.3, Libreria Progetto Publ., Padova.
- Boccotti P., 1989, On mechanics of irregular gravity waves, Atti Acc. Naz. Lincei, Memorie (Trans. Nat. Acc. Lincei), VIII, 19.
- Boccotti P. et al., 1993-a, A field experiment on the mechanics of irregular gravity waves, J. Fluid Mech., 252.
- Boccotti P. et al., 1993-b, An experiment at sea on the reflection of the wind waves, Ocean Engng., 20.
- Hasselmann K. et al., 1973, Measurements of wind wave growth and swell decay during the Joint North Sea Wave Project (JONSWAP), Deut. Hydrogr. Zeit., A-8.
- Longuet-Higgins M.S., 1963, The effects of non-linearities on statistical distributions in the theory of sea waves, J. Fluid Mech., 17.
- Mitsuyasu H. et al., 1975, Observation of directional spectrum of ocean

waves using a clover-leaf buoy, *J. Phys. Oceanography*, 5.

Penny W.G. and Price A.T., 1952, The diffraction theory of sea waves by breakwaters, *Phil. Trans. Roy. Soc.*, A-244.

Phillips O.M., 1967, The theory of wind generated waves, *Adv. in Hydroscience*, 4.